Interstellar polarization and grain alignment: the role of iron and silicon

N.V. Voshchinnikov[1,2,3], Th. Henning[1], M.S. Prokopjeva[2], and H.K. Das[4]

[1] Max-Planck-Institut für Astronomie, Königstuhl 17, D-69117 Heidelberg, Germany, e-mail: voshchinnikov@mpia.de
[2] Sobolev Astronomical Institute, St. Petersburg University, Universitetskii prosp. 28, St. Petersburg, 198504 Russia, e-mail: nvv@astro.spbu.ru
[3] Isaac Newton Institute of Chile, St. Petersburg Branch
[4] IUCAA, Post Bag 4, Ganeshkhind, Pune 411 007, India

ABSTRACT

We compiled the polarimetric data for a sample of lines of sight with known abundances of Mg, Si, and Fe. We correlated the degree of interstellar polarization P and polarization efficiency (the ratio of P to the colour excess $E(B - V)$ or extinction A_V) with dust phase abundances. We detect an anticorrelation between P and the dust phase abundance of iron in non silicate–containing grains [Fe(rest)/H]$_d$, a correlation between P and the abundance of Si, and no correlation between $P/E(B - V)$ or P/A_V and dust phase abundances. These findings can be explained if mainly the silicate grains aligned by the radiative mechanism are responsible for the observed interstellar linear polarization.

1. Introduction

The modelling of interstellar polarization includes light scattering calculations for aligned non-spherical particles. It is usually performed for particles of simple shapes (infinite cylinders or homogeneous spheroids) and the particles are very often assumed to be perfectly aligned (Mathis 1986; Kim & Martin 1995; Draine & Fraisse 2009). The reasons for these simplifications are a poor knowledge of alignment mechanisms (see Lazarian 2009, for a recent review) and the impossibility of light scattering calculations for complex aggregate particles of intermediate and large sizes (Michel et al. 1996; Farafonov & Il'in 2006; Borghese et al. 2007; Min 2009).

According to standard concepts (Krügel 2003; Whittet 2003), the alignment of interstellar grains may be magnetic or radiative. Magnetic alignment occurs if pure iron or iron components in dust grains interact with the magnetic field. Radiative torque alignment (RAT alignment) arises from an azimuthal asymmetry of the light scattering by non-spherical particles. Magnetic inclusions can enhance RAT alignment (Lazarian & Hoang 2008). The amount of iron in dust grains can be found from dust phase abundances. Using them, we can estimate the grain composition and, as a consequence, the scattering and polarizing properties of interstellar dust.

In this paper, we analyse the relation between the interstellar polarization and dust phase abundances of Mg, Si, and Fe previously compiled by Voshchinnikov & Henning (2010, VH10). We assume that all silicon and magnesium and a part of iron are incorporated into amorphous silicates. We correlate the amount of the remaining iron as well as dust phase abundances of Mg, Si, and Fe with the polarization degree P or polarization efficiency (the ratio of P to the colour excess $E(B - V)$ or extinction A_V) and draw some conclusions on grains producing interstellar polarization and favourite alignment mechanism.

2. Polarization and alignment mechanisms

The fact that interstellar grains polarize starlight has important implications. It requires the simultaneous fulfilment of the following conditions in a given direction.

1. Dust grains must be non-spherical.
2. Dust grains must have sizes close to the wavelength of incident radiation because big particles do not polarize the transmitted radiation even if they are perfectly orientated (Voshchinnikov et al. 2000).
3. Dust grains must have specific magnetic properties to interact with the interstellar magnetic field.
4. Dust grains must be aligned.
5. The direction of alignment must not coincide with the line of sight.
6. The distribution of aligned grains along the line of sight must be quite regular to exclude the cancellation of polarization.

The most discussed item is the alignment mechanism. A very popular alignment mechanism is the magnetic alignment (Davis-Greenstein (DG) type orientation, Davis & Greenstein 1951) based on the paramagnetic relaxation of grain material containing about one percent of iron impurities. The DG mechanism requires a stronger magnetic field than average galactic magnetic field ($\sim 3 - 5\,\mu$G; Heiles & Crutcher 2005). Because of this problem, it has been suggested that the polarizing grains contain small clusters of iron, iron sulfides, or iron oxides with superparamagnetic or ferromagnetic properties (Jones & Spitzer 1967). This leads to an enhancement of the imaginary part of the magnetic susceptibility of grain material χ'' by a factor $10 - 100$ and alignment can occur through the DG mechanism. This scenario is supported by laboratory experiments (Djouadi et al. 2007; Belley et al. 2009). A significant enhancement of χ'' is also possible in mixed MgO/FeO/SiO grains (Duley 1978) or in

H_2O ice mantle grains containing magnetite (Fe_3O_4) precipitates (Sorrell 1994, 1995).

A very important factor of any alignment mechanism is grain rotation. The faster it is, the more effective the grain alignment should be. The DG mechanism assumes thermally rotating grains. Purcell (1979) suggested a mechanism of supra-thermal spin alignment ("pinwheel" mechanism) where the grains are spun up to very high velocities as a result of the desorption of H_2 molecules from their surfaces.

Fast rotation can also arise because of radiation torques when asymmetrical grains scatter the radiation (Dolginov et al. 1979; Draine & Weingartner 1997), which can lead to grain alignment in an anisotropic radiation field. Radiation torque is a manifestation of the radiation pressure force possessing a transversal component directed perpendicular to the direction of the incident radiation. This component was measured in laboratory experiments (Abbas et al. 2004; Krauß & Wurm 2004). It can be easily calculated for cylindrical (Voshchinnikov & Il'in 1983) and spheroidal (Voshchinnikov 1990; Il'in & Voshchinnikov 1998) grains and estimated for fluffy aggregates (Kimura & Mann 1998). The transversal component is larger for dielectric particles and plays an important role in the motion of interplanetary and circumstellar grains (Il'in & Voshchinnikov 1998; Kimura et al. 2002; Kocifaj & Klačka 2004).

The theory of RAT alignment is well developed (Lazarian & Hoang 2007). Recent observations of interstellar polarization in the vicinity of luminous stars (Andersson & Potter 2010; Matsumura et al. 2011; Andersson et al. 2011) have been used for confirmation of the RAT alignment mechanism. However, the discussed models are phenomenological, they are not based on correct light scattering calculations of interstellar polarization. One of the reasons is that the alignment function for the RAT mechanism is unknown. Another reason is a requirement of advanced light scattering methods because fast rotation can only occur for grains of very specific (helical) shape (Dolginov et al. 1979; Lazarian & Hoang 2007). This is highly improbable from the point of view of grain growth in the interstellar medium.

In any event, since both magnetic alignment and radiative alignment depend on iron inclusions, we can expect that polarization and/or polarization efficiency should increase with the growth of iron fraction in dust grains. A goal of our investigation is to check this suggestion using the available data on interstellar polarization and element abundances.

3. Results and discussion

We compiled the polarimetric data for a sample of 196 targets with known dust phase abundances collected in VH10. Polarimetric observations of 13 stars in the V band were performed by one of the authors (HKD) in October 2011 at a 2m telescope of the IUCAA Girawali Observatory (Pune, India). The polarization degree P in percent with 1σ error and the corresponding reference are given in Table 1[1] (columns 9 and 13) in the appendix. The total number of stars with measured polarization is 172. Columns 10 and 11 contain the ratios of P to the colour excess $E(B − V)$ and visual extinction A_V[2], which characterizes the polarization efficiency of the interstellar medium in a given direction. In Table 1, the extinction A_V and the ratio
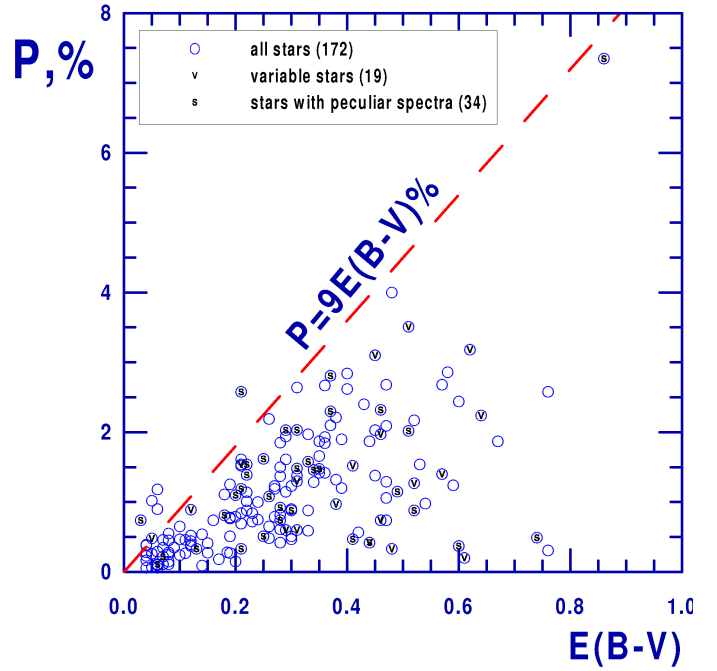

Fig. 1. Polarization according to colour excess for 172 stars from Table 1. Variable stars and stars with peculiar spectra are marked. The straight line shows the empirical upper limit for interstellar polarization (Serkowski et al., 1975).

$P/E(B − V)$ were calculated assuming 1σ error for $E(B − V)$ equal to 0.01.

We marked stars with a peculiar spectrum ('s') and variable stars ('v'). For these, a part of the observed polarization may be intrinsic. However, the positions of these stars on the diagram P vs. $E(B − V)$ do not look unusual (see Fig. 1). In the direction of variable stars or stars with peculiar spectrum where the interstellar polarization was determined from polarization of surrounding stars, we used this interstellar polarization (labelled 'i'). The polarimetric data are mainly related to the visual part of spectrum (V band). For stars marked 'm' the value of the maximum polarization P_{max} is given. The major part of observations was taken from the catalogues of Heiles (2000), Serkowski et al. (1975), and Efimov (2009). In the latter case, we used P_{max} obtained for the Serkowski curve approximated according to Whittet et al. (1992).

Voshchinnikov & Henning (2010) found a sharp distinction in abundances of Mg, Si, and Fe for sightlines located at low ($|b| < 30°$) and high ($|b| > 30°$) galactic latitudes. For high-latitude stars the ratios Mg/Si and Fe/Si in dust are close to 1.5. For disk stars these ratios are reduced to ~ 1.2 and ~ 1.05 for Mg and Fe, respectively. The derived numbers indicate that the dust grains cannot be just a mixture of only olivine ($Mg_{2x}Fe_{2−2x}SiO_4$) and pyroxene ($Mg_yFe_{1−y}SiO_3$) silicates (here $0 \leq x, y \leq 1$). Some amount of magnesium or iron (or both) should be embedded into other materials.

Based on the discussion of alignment mechanisms (Sect. 2), we suggest that the interstellar polarization is probably be related to the amount of iron in dust grains. We assume that *all silicon and all magnesium are embedded into amorphous silicates of olivine composition* ($Mg_{2x}Fe_{2−2x}SiO_4$, where $x =$

$[Mg/H]_d/(2[Si/H]_d)$ as is a part of iron. The remaining part of Fe can be found as

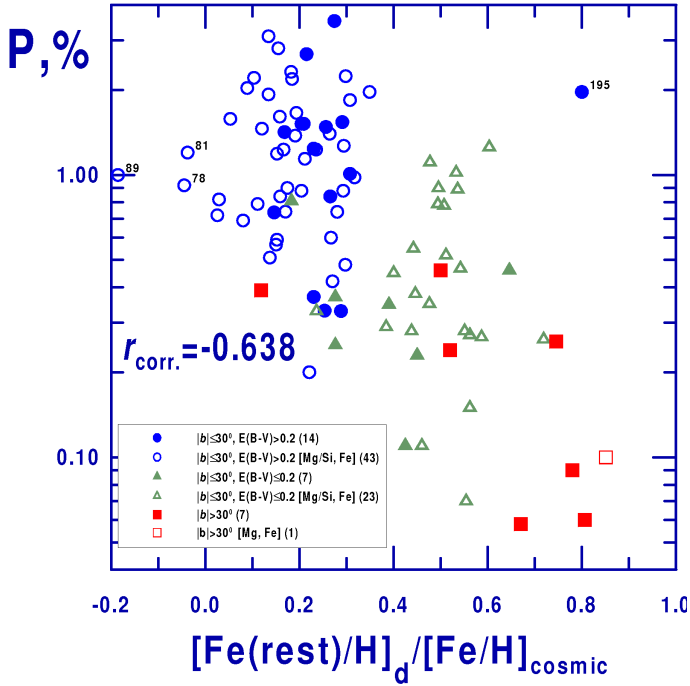$$[Fe(rest)/H]_d = [Fe/H]_d - (2 \, [Si/H]_d - [Mg/H]_d). \qquad (1)$$

Fig. 2. Polarization of 95 stars according to the remaining dust phase abundance of Fe as given by Eq. (1) normalized to the cosmic abundance of iron. Halo stars with $|b| > 30°$ and disk stars with $|b| \le 30°$ and low ($E(B-V) \le 0.2$) and high ($E(B-V) > 0.2$) reddening are shown with different symbols. Filled symbols correspond to sightlines where the abundances of three elements (Mg, Si, and Fe) are measured. Open symbols correspond to sightlines where the abundances of two elements (Fe and Mg or Si) are known. The number of stars is indicated in parentheses in the legend.

It is expected to be in the form of various iron oxides (FeO, Fe_2O_3, Fe_3O_4) and/or metallic iron, which confers magnetic properties to the grains.

Our choice of Mg-rich silicates with the olivine stoichiometry is based on the theoretical and observational studies of dust composition in circumstellar environments (Gail 2010; Molster et al. 2010; Sturm et al. 2010) and on the interpretation of the observed interstellar silicate absorption profiles (Min et al. 2007; van Breemen et al. 2011). Probably the single exception is the oxygen-rich AGB star T Cep, whose peak wavelength in the IR features suggests the presence of Fe-rich silicates (Niyogi et al. 2011).

Using Eq. (1), we calculated the dust phase abundance of Fe incorporated into non-silicate materials $[Fe(rest)/H]_d$ (see column 13 in Table 1). Then these abundances were normalized to the solar (cosmic) abundance of iron ($[Fe/H]_\odot = 31.6$ ppm, Asplund et al. 2009)[3] and we correlated them with the polarization and polarization efficiency. The results are shown in Figs. 2 and 3 and in Table 2 (rows 1 − 3). The abundances of the three

---

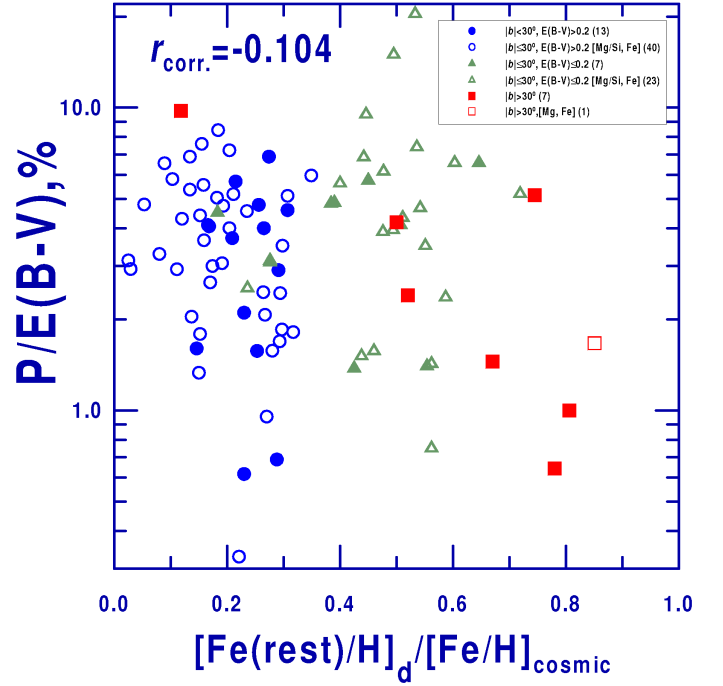[3] The normalization with $[Fe/H]_{cosmic}$ was performed to obtain convenient units.

elements Mg, Si, and Fe were measured only for the 28 targets with known polarization. They are plotted in the figures using filled symbols. To increase the sample volume, we calculated $[Fe(rest)/H]_d$ for sightlines where the abundances of two elements (Fe and Mg or Si) were known. In this case, we use the average abundance of the third (lacking) element as given in rows 2 − 5 of Table 2 in VH10. These data are shown by open symbols in Figs. 2 and 3. Clearly, the amount of Fe in non-silicates is quite high, especially for low-reddened ($E(B - V) \lesssim 0.2$) and halo ($|b| > 30°$) stars. There is also a tendency for a decline in polarization (see Fig. 2) with transition from high-reddened to low-reddened stars, which likely reflects a fall of the column density of polarizing grains. An exception is the sightline towards the star N 195 (CPD −59 2603), where the dust phase abundance of Si is very low. There are also three targets (NN 78, 81, and 89) where the calculated values of $[Fe(rest)/H]_d$ are negative. We excluded these four stars from the correlation analysis (rows 1 − 3 in Table 2).

As indicated in Fig. 2, there is a negative correlation between the polarization degree P and the amount of remaining iron. This is inconsistent with the common suggestion about the great role of iron-rich grains in the production of polarization. Because P is proportional to the column density of polarizing grains, we can conclude that *the increase of the iron content in non-silicate grains does not enhance polarization*. These particles may be spherical, very large or very small in comparison with radiation wavelength, or they may be less aligned. It is also important that metallic iron or iron oxides have high refractive indices, and particles consisting of these materials scatter less radiation compared with (Mg,Fe)-silicates, which prevents radiative torques. Therefore, we can conservatively estimate that the radiative alignment is the favourite alignment mechanism of the interstellar grains.
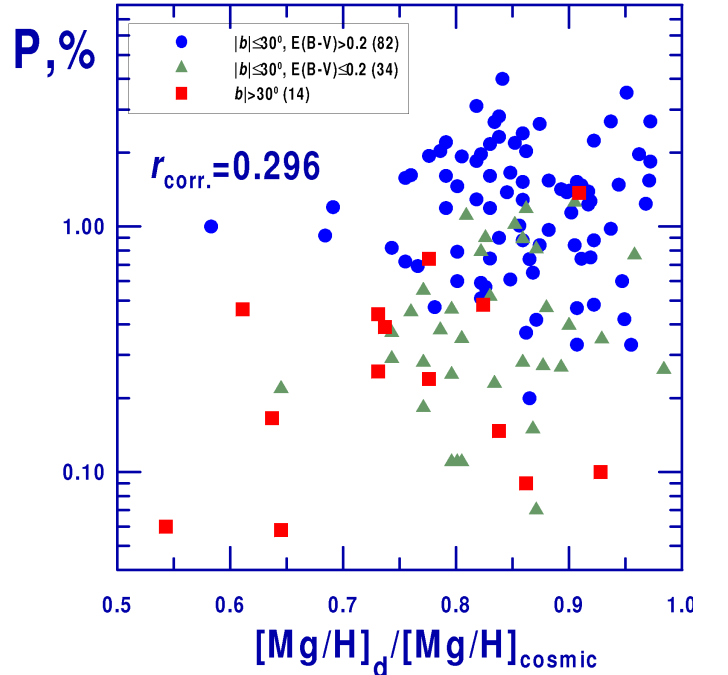
Because in calculating $[Fe(rest)/H]_d$ we removed all Si and Mg and a part of Fe from the dust phase, we expect a positive

Fig. 3. Same as in Fig. 2, but now for polarization efficiency $P/E(B − V)$.

Table 2. Pearson correlation coefficients between polarization, extinction, and element abundances in the dust phase.

Parameters and Figure	$N_{\rm stars}$	$r_{\rm corr.}$	Comment
$\log P$ vs. $[{\rm Fe(rest)/H}]_{\rm d}$ $/[{\rm Fe/H}]_{\rm cosmic}$, Fig. 2	91	–0.638	Polarizing grains are not iron-rich non-silicates
$\log P/E(B-V)$ vs. $[{\rm Fe(rest)/H}]_{\rm d}/[{\rm Fe/H}]_{\rm cosmic}$, Fig. 3	91	–0.104	No correlation
$\log P/A_V$ vs. $[{\rm Fe(rest)/H}]_{\rm d}$ $/[{\rm Fe/H}]_{\rm cosmic}$	69	0.137	”
$\log P$ vs. $[{\rm Fe/H}]_{\rm d}$ $/[{\rm Fe/H}]_{\rm cosmic}$, Fig. 4	121	0.351	Weak correlation
$\log P/E(B-V)$ vs. $[{\rm Fe/H}]_{\rm d}$ $/[{\rm Fe/H}]_{\rm cosmic}$	121	0.013	No correlation
$\log P/A_V$ vs. $[{\rm Fe/H}]_{\rm d}$ $/[{\rm Fe/H}]_{\rm cosmic}$	98	–0.117	”
$\log P$ vs. $[{\rm Mg/H}]_{\rm d}$ $/[{\rm Mg/H}]_{\rm cosmic}$, Fig. 5	130	0.296	Weak correlation
$\log P/E(B-V)$ vs. $[{\rm Mg/H}]_{\rm d}$ $/[{\rm Mg/H}]_{\rm cosmic}$	130	–0.050	No correlation
$\log P/A_V$ vs. $[{\rm Mg/H}]_{\rm d}$ $/[{\rm Mg/H}]_{\rm cosmic}$	94	–0.174	”
$\log P$ vs. $[{\rm Si/H}]_{\rm d}$ $/[{\rm Si/H}]_{\rm cosmic}$, Fig. 6	34	0.736	Polarizing grains are silicates
$\log P/E(B-V)$ vs. $[{\rm Si/H}]_{\rm d}$ $/[{\rm Si/H}]_{\rm cosmic}$	34	0.116	No correlation
$\log P/A_V$ vs. $[{\rm Si/H}]_{\rm d}$ $/[{\rm Si/H}]_{\rm cosmic}$	16	0.013	”
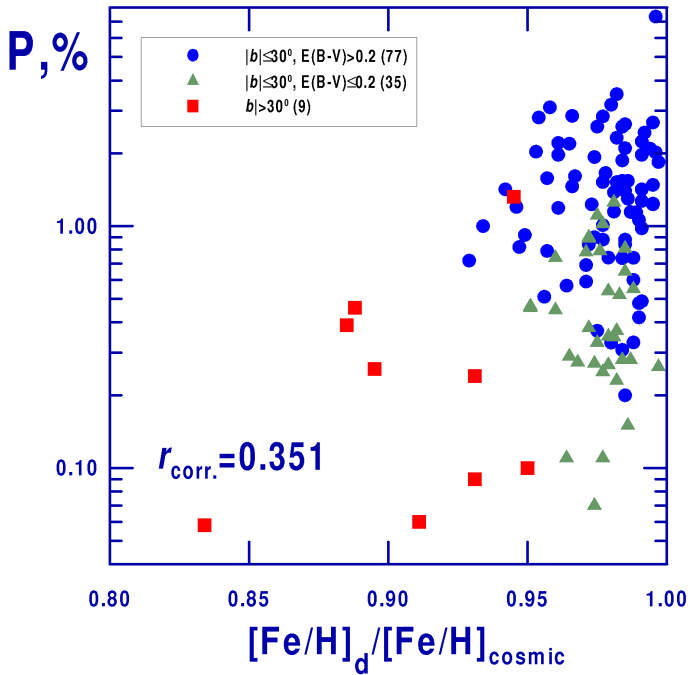
Fig. 4. Interstellar polarization according to dust phase abundance of iron. Halo stars with $|b| > 30°$ and disk stars with $|b| \le 30°$ and low ($E(B - V) \le 0.2$) and high ($E(B - V) > 0.2$) reddening are shown with different symbols. The number of stars is indicated in parentheses in the legend.

Fig. 5. Same as in Fig. 4, but now for magnesium.

correlation between the polarization and the abundances of the eliminated elements. Figures 4 – 6 show the dependence of interstellar polarization on dust phase abundances of iron, magnesium, and silicon. Evidently, there is only a weak correlation between P and $[{\rm Fe/H}]_{\rm d}$ or $[{\rm Mg/H}]_{\rm d}$ and a strong correlation between P and $[{\rm Si/H}]_{\rm d}$. Therefore, we can establish that *polarization is more likely produced by silicates*. These findings are evidence in favour of the assumption of Mathis (1986) that only the silicate grains are aligned and contribute to the observed polarization, while the carbonaceous grains are either spherical or randomly aligned. Note that a poor alignment of carbonaceous grains compared with silicate grains also follows from the consideration of disalignment caused by thermal flipping or discrete

charging (Weingartner 2006). Another verification of this suggestion is the absence of any correlation between the polarization efficiency $P/E(B - V)$ or P/A_V and dust phase abundances of elements (see Table 2 and Fig. 3). This is because dust grains of all types (silicate, carbonaceous, iron-rich, etc.) contribute to the observed extinction A_V and most likely to the colour excess $E(B - V) = A_B - A_V$, while only the silicates seems to be responsible for the observed polarization. Thus, the absence of correlation between the ratio of the total to selective extinction R_V and the wavelength of maximum polarization $\lambda_{\rm max}$ observed in many cases (e.g., Whittet et al. 2001; Andersson & Potter 2007) can be easily understood.

4. Conclusions

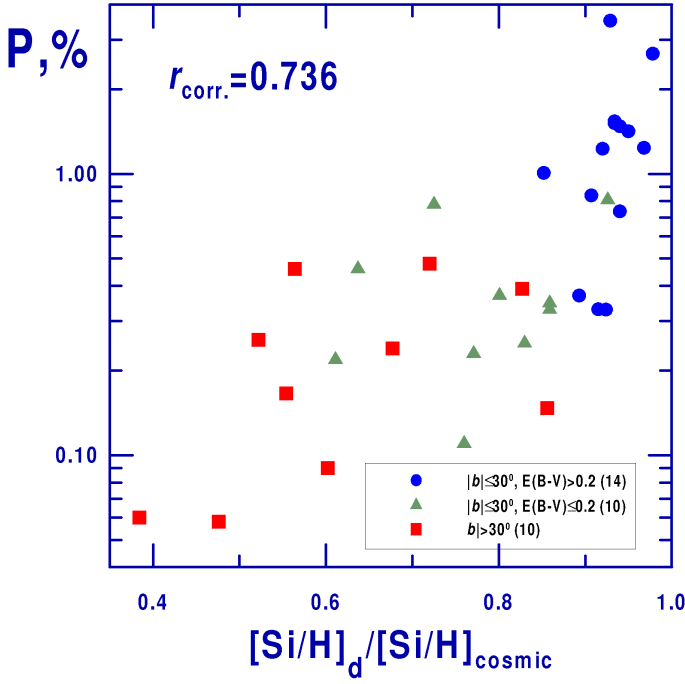The main results of the paper can be formulated as follows.

Fig. 6. Same as in Fig. 4, but now for silicon.

1. We compiled the polarimetric data for a sample of 196 lines of sight with known dust phase abundances of Mg, Si, and Fe collected in Voshchinnikov & Henning (2010). The total number of stars with measured polarization is 172. Polarimetric observations of 13 stars are presented for the first time in this paper.

2. Assuming that all Si and Mg and a part of Fe are incorporated into amorphous silicates of olivine composition, we calculated the dust phase abundance of the remaining iron. The fraction of iron not included in silicates $[Fe(rest)/H]_d$ is quite high: changing from ~ 0.1 of cosmic abundance of Fe for reddened disk ($|b| < 30°$, $E(B - V) > 0.2$) stars to ~ 0.8 for halo ($|b| > 30°$) stars.

3. We detect an anticorrelation between P and $[Fe(rest)/H]_d$ ($r_{corr.} = -0.638$) and a correlation between P and dust phase abundances of Si ($r_{corr.} = 0.736$). We conclude that it is more likely that polarization is produced by silicates and is not produced by iron-rich non-silicate grains. Because silicate grains scatter more radiation than grains of other types (carbonaceous, iron oxides, etc.), these findings can be interpreted in favour of the radiative alignment of interstellar grains.

4. We found no correlation between the polarization efficiency (the ratio of P to the colour excess $E(B - V)$ or extinction A_V) and the dust phase abundances of Mg, Si, or Fe. This fact can be explained if we assume that dust grains of all types contribute to A_V and $E(B - V)$, while only the silicates are responsible for the observed polarization.

A more reliable decision about the contribution of the grains of different types to the observed linear interstellar polarization and the grain alignment can be reached after detailed modelling.

References

Abbas, M.M., Craven, P.D., Spann, J.F. et al. 2004, ApJ, 614, 781
Andersson, B.-G., & Potter, S.B. 2007, ApJ, 665, 369
Andersson, B.-G., & Potter, S.B. 2010, ApJ, 720, 1045
Andersson, B.-G., & Wannier, P.G. 1997, ApJ, 491, L103
Andersson, B.-G., Pintado, O., Potter, S.B., Straižys, V., & Charcos-Llorens, M. 2011, A&A, 534, A19
Asplund, M., Grevesse, N., Sauval, A.J., & Scott, P. 2009, ARA&A, 47, 481
Belley, F., Ferré, E.C., Martín-Hernández, F. et al. 2009, Earth Plan. Sci. Lett., 284, 516
Borghese, F., Denti, P., & Saija, R. Scattering by model non-spherical particles, Second Edition (Heidelberg: Springer)
Das, H.K., Voshchinnikov N.V., & Il'in, V.B. 2010, MNRAS, 404, 265
Davis, L., & Greenstein, J.L. 1951, ApJ, 114, 206
Djouadi, G., Gattacceca, J., d'Hendecourt, L., Rochette, P., Jones, A.P., Davoisne, C., Leroux, H., & Borg, J. 2007, A&A, 468, L9
Dolginov, A.Z., Gnedin, Yu.N., & Silant'ev, N.A. 1979, Propagation and Polarization of Radiation in Cosmic Medium (Moscow: Nauka)
Duley, W.W. 1978, ApJ, 219, L129
Draine, B.T., & Fraisse, A.A. 2009, ApJ, 626, 1
Draine, B.T., & Weingartner, J.C. 1997, ApJ, 480, 663
Efimov, Yu. S. 2009, Bull. CrAO, 105, 82
Elias, N.M., Koch, R.H., & Pfeiffer, R.J. 2008, A&A, 489, 911
Farafonov, V.G., & Il'in, V.B. 2006, in Light Scattering Reviews, ed. A.A. Kokhanovsky, Springer, 1, 125
Fitzpatrick, E.L., & Massa, D.L. 2007, ApJ, 663, 320
Gail, H.-P. 2010, in Astromineralogy, Second Edition, ed. Th. Henning, Springer, Lect. Notes in Phys., 815, 61
Ghosh, K., Iyengar, K.V.K., Ramsey, B.D., & Austin, R.A. 1999, AJ, 118, 1061
Harries, T.J., Howarth, I.D., & Evans, C.J. 2002, MNRAS, 337, 341
Heiles, C. 2000, AJ, 119, 923
Heiles, C., & Crutcher, R. 2005, in Cosmic Magnetic Fields, ed. R. Wielebinski, & R. Beck, Lect. Notes Phys., 664, 137
Jones, R.V., & Spitzer, L. 1967, ApJ, 147, 943
Il'in, V.B., & Voshchinnikov, N.V. 1998, A&AS, 128, 187
Kim, S.-H., & Martin, P.G. 1995, ApJ, 444, 293
Kimura, H., & Mann, I. 1998, JQSRT, 60, 425
Kimura, H., Okamoto, H., & Mukai, T. 2002, Icarus, 157, 349
Kocifaj, M., & Klačka, J. 2004, JQSRT, 89, 165
Krauß, O., & Wurm, G. 2004, JQSRT, 89, 179
Krügel, E. 2003, The Physics of Interstellar Dust (London: Institute of Physics Publishing)
Larson, K.A., Whittet, D.C.B. & Hough, J.H. 1996, ApJ, 472, 755
Lazarian, A. 2009, in Cosmic Dust – Near and Far, ed. Th. Henning et al., ASP Conf. Ser., 414, 482
Lazarian, A., & Hoang, T. 2007, MNRAS, 378, 910
Lazarian, A., & Hoang, T. 2008, ApJ, 676, L25
Leroy, J.L., & Le Borgne, J.F. 1987, A&A, 186, 322
Marraco, H.G., Vega, E.I., & Vrba, F.J. 1993, AJ, 105, 258
Martin, P.G., Clayton, G.C., & Wolff, M.J. 1999, ApJ, 510, 905
Mathis, J.S. 1986, ApJ, 308, 281
Matsumura, M., Kameura, Y., Kawabata K.S. et al. 2011, PASJ, 63, L43
McDavid, D. 2000, AJ, 119, 352
Michel, B., Henning, Th., Stognienko, R., & Rouleau, F. 1996, ApJ, 468, 834
Min, M. 2009, in Cosmic Dust – Near and Far, ed. Th. Henning et al., ASP Conf. Ser., 414, 356
Min, M., Waters, L.B.F.M., de Koter, A., Hovenier, J.W., Keller, L.P., & Markwick-Kemper, F. 2007, A&A, 462, 667
Molster, F.J., Waters, L.B.F.M., & Kemper, F. 2010, in Astromineralogy, Second Edition, ed. Th. Henning, Springer, Lect. Notes in Phys., 815, 143
Niyogi, S.G., Speck, A.K., & Onaka, T. 2011, ApJ, 733:93
Oudmaijer, R.D., & Drew, J.E. 1999, MNRAS, 305, 166
Patriarchi, P., Morbidelli, L. & Perinotto, M. 2003, A&A, 410, 905
Poeckert, R., Bastien, P., & Landstreet, J.D. 1979, AJ, 84, 812
Purcell, E.M. 1979, ApJ, 231, 404
Roche, P., Larionov, V., Tarasov, A.E. et al. 1997, A&A, 322, 139
Serkowski, K., Mathewson, D.S., & Ford, V.L. 1975, ApJ, 196, 261
Sorrell, W.H. 1994, MNRAS, 268, 40
Sorrell, W.H. 1995, MNRAS, 273, 187
Sturm, B., Bouwman, J., Henning, Th. et al. 2010, A&A, 518, L129
Valencic, L.A., Clayton, J.C. & Gordon, K.D. 2004, ApJ, 616, 912
van Breemen, J.M., Min, M., Chiar, J.E. et al. 2011, A&A, 526, A152
Vega, E.I., Orsatti, A.M., & Marraco, H.G. 1994, AJ, 108, 1834

Vink, J.S., Davies, B., Harries, T.J., Oudmaijer, R.D., & Walborn, N.R. 2009, A&A, 505, 743

Voshchinnikov N.V. 1990, SvA., 33, 429

Voshchinnikov, N.V., & Henning, Th. 2010, A&A, 517, A45 (VH10)

Voshchinnikov, N.V., & Il'in, V.B. 1983, SvA Lett., 9, 101

Voshchinnikov, N.V., Il'in, V.B., Henning, Th., Michel, B., & Farafonov, V.G. 2000, JQSRT, 65, 877

Wegner, W. 2002, BaltA, 11, 1

Wegner, W. 2003, AN, 324, 219

Weingartner, J.C. 2006, ApJ, 647, 390

Weitenbeck, A.J. 2008, AcAstr, 58, 433

Whittet, D.C.B. 2003, Dust in the Galactic Environments, Second Edition (Bristol: Institute of Physics Publishing)

Whittet, D.C.B., Martin, P.G., Hough, J.H. et al. 1992, ApJ, 386, 562

Whittet, D.C.B., Gerakines, P.G., Hough, J.H., & Shenoy, S.S. 2001, ApJ, 547, 872

Appendix

Table 1. Polarization of stars with known dust phase abundances.

N (1)	Star (2)	l (3)	b (4)	Spectrum (5)	D, pc (6)	E(B − V) (7)	A_V (8)	P, % (9)	P/E(B − V), % (10)	P/A_V, % (11)	[Fe(rest)/H]$_d$ (12)	Reference (13)
1	HD 1383	119.02	–0.89	B1II	2702	0.47	1.30 ± 0.12	1.29 ± 0.20	2.74 ± 0.48	0.99 ± 0.24	· · ·	(1)
2v	HD 5394	123.58	–2.15	B0IVpe	188	0.12	· · ·	0.89 ± 0.07	7.42 ± 1.20	· · ·	16.95 ± 8.48	(2)
3	HD 12323	132.91	–5.87	ON9V	3586	0.21	0.61 ± 0.08	1.52 ± 0.18	7.24 ± 1.20	2.50 ± 0.64	6.44 ± 5.15	(1)
4	HD 13268	133.96	–4.99	O8V	2391	0.36	1.09 ± 0.12	2.67 ± 0.20	7.42 ± 0.76	2.46 ± 0.45	· · ·	(1)
5s	HD 13745	134.58	–4.96	O9.7IIn	1900	0.37	1.14 ± 0.14	2.81 ± 0.20	7.59 ± 0.75	2.46 ± 0.48	4.89 ± 6.02	(1)
6	HD 14434	135.08	–3.82	O6.5V	4108	0.48	1.23 ± 0.10	4.00 ± 0.20	8.33 ± 0.59	3.24 ± 0.43	· · ·	(1)
7s	HD 15137	137.46	+7.58	O9.5II-IIIn	3300	0.31	1.10 ± 0.13	2.032 ± 0.0414	6.55 ± 0.34	1.85 ± 0.25	2.81 ± 7.19	(3)
8	HD 18100	217.93	–62.73	B5II-III	3100	0.05	· · ·	0.257 ± 0.0367	5.14 ± 1.76	· · ·	23.55 ± 19.70	(3)
9	HD 21856	156.32	–16.75	B1V	500	0.19	· · ·	0.78 ± 0.20	4.11 ± 1.27	· · ·	16.02 ± 16.34	(1)
10	HD 22586	264.19	–50.36	B2III	2020	0.06	· · ·	0.100 ± 0.035	1.67 ± 0.86	· · ·	26.88 ± 11.87	(1)
11	HD 22928	150.28	–5.77	B5III	160	0.05	· · ·	0.262 ± 0.069	5.24 ± 2.43	· · ·	22.73 ± 6.33	(1)
12	HD 22951	158.92	–16.70	B0.5V	320	0.19	· · ·	0.766 ± 0.099	4.03 ± 0.73	· · ·	· · ·	(1)
13v	HD 23180	160.36	–17.74	B1IVSB	219	0.29	0.91 ± 0.10	0.6 ± 0.2	2.07 ± 0.76	0.66 ± 0.29	8.44 ± 3.22	(4)
14	HD 23478	160.76	–17.42	B3IV	240	0.28	· · ·	1.5 ± 0.05	5.36 ± 0.37	· · ·	· · ·	(4)
15	HD 24190	160.39	–15.90	B2V	550	0.30	· · ·	0.51 ± 0.20	1.70 ± 0.72	· · ·	· · ·	(1)
16m	HD 24398	162.29	–16.69	B1Ib	301	0.27	0.71 ± 0.07	1.23 ± 0.088	4.56 ± 0.49	1.73 ± 0.29	7.42 ± 3.07	(5)
17im	HD 24534	163.08	–17.14	O9.5pe	590	0.59	2.05 ± 0.21	1.24 ± 0.01	2.10 ± 0.05	0.61 ± 0.07	7.27 ± 2.23	(6)
18	HD 24760	157.35	–10.09	B0.5IV	165	0.11	· · ·	0.267 ± 0.063	2.43 ± 0.79	· · ·	18.54 ± 8.26	(1)
19m	HD 24912	160.37	–13.10	O7V	421	0.35	1.00 ± 0.21	1.42 ± 0.03	4.06 ± 0.20	1.42 ± 0.32	5.30 ± 2.72	(7)
20	HD 27778	172.76	–17.39	B3V	262	0.36	0.96 ± 0.08	1.841 ± 0.0312	5.11 ± 0.23	1.91 ± 0.19	9.69 ± 1.78	(3)
21v	HD 28497	208.78	–37.40	B2Vne	483	0.05	· · ·	0.48 ± 0.05	9.60 ± 2.92	· · ·	· · ·	(2)
22m	HD 30614	144.07	14.04	O9.5Ia	963	0.29	0.87 ± 0.13	1.61 ± 0.02	5.55 ± 0.26	1.84 ± 0.29	4.99 ± 6.67	(8)
23	HD 34029	162.59	+4.57	G8III+G0III	13	0.01	· · ·	· · ·	· · ·	· · ·	19.46 ± 6.34	
24	HD 34816	214.83	–26.24	B0.5IV	260	0.05	· · ·	· · ·	· · ·	· · ·	· · ·	
25	HD 34989	194.62	–15.61	B1V	490	0.10	0.27 ± 0.06	0.65 ± 0.20	6.50 ± 2.65	2.37 ± 1.27	· · ·	(1)
26	HD 35149	199.16	–17.86	B1V	295	0.12	0.39 ± 0.07	0.37 ± 0.20	3.08 ± 1.92	0.94 ± 0.67	8.73 ± 7.07	(1)
27	HD 35715	200.09	–17.22	B2IV	370	0.04	· · ·	0.28 ± 0.05	7.00 ± 3.00	· · ·	· · ·	(1)
28	HD 36486	203.86	–17.74	O9.5II	281	0.08	· · ·	0.11 ± 0.10	1.38 ± 1.42	· · ·	13.44 ± 4.03	(1)
29	HD 36822	195.40	–12.29	B0.5IV-V	330	0.08	0.21 ± 0.07	0.28 ± 0.10	3.50 ± 1.69	1.33 ± 0.90	17.42 ± 9.05	(1)
30m	HD 36861	195.05	–12.00	O8IIIf	550	0.09	0.22 ± 0.08	0.35 ± 0.113	3.89 ± 1.69	1.58 ± 1.07	15.05 ± 9.45	(9)
31v	HD 37021	209.01	–19.38	B0V	678	0.48	2.80 ± 0.18	0.33 ± 0.08	0.69 ± 0.18	0.12 ± 0.04	9.10 ± 4.05	(10)
32	HD 37043	209.52	–19.58	O9III	406	0.07	· · ·	0.11 ± 0.02	1.57 ± 0.51	· · ·	14.55 ± 8.32	(1)
33m	HD 37061	208.92	–19.27	B0.5 V	476	0.53	2.41 ± 0.11	1.54 ± 0.077	2.91 ± 0.20	0.64 ± 0.06	9.20 ± 2.11	(5)
34	HD 37128	205.21	–17.24	B0Iab	412	0.04	· · ·	0.23 ± 0.02	5.75 ± 1.94	· · ·	14.23 ± 5.79	(1)
35v	HD 37367	179.04	–1.03	B2 V SB	273	0.38	1.27 ± 0.09	0.97 ± 0.20	2.55 ± 0.59	0.76 ± 0.21	· · ·	(1)
36	HD 37468	206.82	–17.34	O9.5V	370	0.06	· · ·	0.29 ± 0.02	4.83 ± 1.14	· · ·	12.13 ± 9.98	(1)
37m	HD 37903	206.85	–16.54	B1.5V	719	0.33	1.30 ± 0.11	1.97 ± 0.01	5.97 ± 0.21	1.51 ± 0.13	11.02 ± 3.65	(7)
38m	HD 38087	207.07	–16.26	B5V	315	0.31	1.80 ± 0.14	2.64 ± 0.01	8.52 ± 0.31	1.47 ± 0.12	· · ·	(8)
39	HD 38666	237.29	–27.10	O9.5V	397	0.06	· · ·	0.060 ± 0.035	1.00 ± 0.75	· · ·	25.48 ± 5.68	(1)
40m	HD 38771	214.51	–18.50	B0Iab	221	0.12	· · ·	0.52 ± 0.075	4.33 ± 0.99	· · ·	16.15 ± 7.42	(5)
41	HD 40111	183.97	+0.84	B0.5II	480	0.18	0.55 ± 0.09	1.11 ± 0.20	6.17 ± 1.45	2.02 ± 0.68	15.08 ± 9.95	(1)
42	HD 40893	180.09	+4.34	B0IV:	2632	0.45	1.22 ± 0.09	1.38 ± 0.18	3.07 ± 0.47	1.13 ± 0.23	6.03 ± 4.94	(1)
43m	HD 41117	189.69	–0.86	B2Ia	909	0.40	1.25 ± 0.15	2.84 ± 0.274	7.10 ± 0.86	2.28 ± 0.49	· · ·	(5)
44s	HD 41161	164.97	+12.89	O8Vn	1400	0.21	0.55 ± 0.17	2.58 ± 0.20	12.29 ± 1.54	4.67 ± 1.81	· · ·	(1)
45m	HD 42087	187.75	+1.77	B2.5Ib	1578	0.37	1.17 ± 0.20	2.10 ± 0.075	5.68 ± 0.36	1.80 ± 0.37	· · ·	(5)

Voshchinnikov et al.: Interstellar polarization and grain alignment

Table 1. continued.

N (1)	Star (2)	l (3)	b (4)	Spectrum (5)	D, pc (6)	E(B − V) (7)	A_V (8)	P, % (9)	P/E(B − V), % (10)	P/A_V, % (11)	[Fe(rest)/H]$_d$ (12)	Reference (13)
46m	HD 43384	187.99	+3.53	B3Ia	1100	0.58	1.77 ± 0.20	2.86 ± 0.05	4.93 ± 0.17	1.61 ± 0.21	⋯	(7)
47	HD 43818	188.49	+3.87	B0II	1623	0.52	1.80 ± 0.13	2.17 ± 0.20	4.17 ± 0.46	1.21 ± 0.20	⋯	(1)
48s	HD 46056	206.34	−2.25	O8V(n)	1670	0.49	1.40 ± 0.08	1.15 ± 0.20	2.35 ± 0.46	0.82 ± 0.19	⋯	(1)
49	HD 46202	206.31	−2.00	O9V	1670	0.47	1.47 ± 0.08	1.06 ± 0.20	2.26 ± 0.47	0.72 ± 0.18	⋯	(1)
50s	HD 47839	202.94	+2.20	O7Ve	313	0.07	⋯	0.219 ± 0.132	3.13 ± 2.33	⋯	⋯	(1)
51	HD 48915	227.23	−8.89	A1V	3	−0.01	⋯	⋯	⋯	⋯	⋯	
52	HD 52266	219.13	−0.68	O9IV	1735	0.26	0.86 ± 0.09	0.65 ± 0.20	2.50 ± 0.87	0.76 ± 0.31	⋯	(1)
53s	HD 53367	223.71	−1.90	B0IV:e	780	0.74	1.76 ± 0.76	0.49 ± 0.01	0.66 ± 0.02	0.28 ± 0.13	⋯	(11)
54	HD 53975	225.68	−2.32	O7.5V	1400	0.185	0.60 ± 0.07	0.28 ± 0.20	1.51 ± 1.16	0.47 ± 0.39	13.84 ± 8.66	(1)
55i	HD 54662	224.17	−0.78	O6.5V	1220	0.26	0.81 ± 0.09	0.481 ± 0.200	1.85 ± 0.84	0.59 ± 0.31	9.39 ± 5.80	(12)
56	HD 57060	237.82	−5.37	O7Iabfp	1870	0.14	0.70 ± 0.09	⋯	⋯	⋯	12.17 ± 11.88	
57	HD 57061	238.18	−5.54	O9II	980	0.10	0.36 ± 0.07	⋯	⋯	⋯	9.66 ± 7.78	
58m	HD 62542	255.92	−9.24	B5V	396	0.36	0.99 ± 0.08	1.42 ± 0.01	3.94 ± 0.14	1.44 ± 0.12	⋯	(7)
59	HD 63005	242.47	−0.93	O6Vf	5200	0.28	0.83 ± 0.55	0.417 ± 0.052	1.49 ± 0.24	0.50 ± 0.39	⋯	(1)
60m	HD 64760	262.06	−10.42	B0.5Ib	510	0.08	0.23 ± 0.07	0.45 ± 0.035	5.63 ± 1.14	1.95 ± 0.75	12.65 ± 10.63	(5)
61	HD 65575	266.68	−12.32	B3IVp	140	0.05	⋯	⋯	⋯	⋯	22.98 ± 6.09	
62s	HD 65818	263.48	−10.28	B2II/IIIn	290	0.06	⋯	0.110 ± 0.035	1.83 ± 0.89	⋯	⋯	(1)
63	HD 66788	245.43	+2.05	O8V	4200	0.20	0.69 ± 0.09	0.79 ± 0.10	3.95 ± 0.70	1.14 ± 0.30	15.62 ± 9.75	(1)
64	HD 66811	255.98	−4.71	O5Ibnf	330	0.05	0.25 ± 0.09	⋯	⋯	⋯	29.64 ± 21.74	
65	HD 68273	262.80	−7.68	WC8+O9I	350	0.03	⋯	⋯	⋯	⋯	17.66 ± 12.07	
66	HD 69106	254.52	−1.33	B0.5II	3076	0.20	0.61 ± 0.12	0.15 ± 0.1	0.75 ± 0.54	0.25 ± 0.21	17.76 ± 7.60	(1)
67	HD 71634	273.32	−11.52	B5III	400	0.13	⋯	⋯	⋯	⋯	⋯	
68s	HD 72754	266.83	−5.82	B2Ia:pshe	690	0.36	⋯	⋯	⋯	⋯	⋯	
69m	HD 73882	260.18	+0.64	O8.5V	759	0.67	2.31 ± 0.09	1.87 ± 0.01	2.79 ± 0.06	0.81 ± 0.04	⋯	(7)
70m	HD 74375	275.82	−10.86	B1.5III	440	0.14	0.53 ± 0.19	0.54 ± 0.035	3.86 ± 0.53	1.02 ± 0.43	⋯	(5)
71	HD 75309	265.86	−1.90	B2Ib/II	2924	0.28	0.95 ± 0.09	0.61 ± 0.10	2.18 ± 0.43	0.64 ± 0.17	⋯	(1)
72m	HD 79186	267.36	+2.25	B5Ia	980	0.40	1.28 ± 0.26	2.62 ± 0.179	6.55 ± 0.61	2.04 ± 0.55	⋯	(5)
73	HD 79351	277.69	−7.37	B2IV-V	140	0.10	⋯	⋯	⋯	⋯	⋯	
74s	HD 88115	285.32	−5.53	B1.5IIn	3654	0.20	⋯	1.10 ± 0.10	5.50 ± 0.78	⋯	⋯	(1)
75	HD 90087	285.16	−2.13	B2/B3III	2716	0.30	0.98 ± 0.12	1.23 ± 0.10	4.10 ± 0.47	1.25 ± 0.26	5.25 ± 5.91	(1)
76	HD 91316	234.89	+52.77	B1Iab	1754	0.04	⋯	0.166 ± 0.025	4.15 ± 1.66	⋯	⋯	(1)
77	HD 91597	286.86	−2.37	B7/B8IV/V	6400	0.27	1.33 ± 0.13	1.19 ± 0.10	4.41 ± 0.53	0.89 ± 0.16	4.81 ± 5.20	(1)
78s	HD 91651	286.55	−1.72	O9V:n	2964	0.28	0.98 ± 0.10	0.92 ± 0.10	3.29 ± 0.47	0.94 ± 0.20	−1.41 ± 6.24	(1)
79s	HD 91824	285.70	+0.07	O7V((f))	2910	0.25	0.77 ± 0.08	1.620 ± 0.164	6.48 ± 0.92	2.10 ± 0.44	⋯	(1)
80	HD 91983	285.88	+0.05	B1III	2910	0.29	0.93 ± 0.12	1.94 ± 0.40	6.69 ± 1.61	2.09 ± 0.70	⋯	(1)
81	HD 92554	287.60	−2.02	O5III	6795	0.39	1.15 ± 0.15	1.20 ± 0.10	3.08 ± 0.34	1.04 ± 0.22	−1.20 ± 8.16	(1)
82	HD 93030	289.60	−4.90	B0V	140	0.04	0.10 ± 0.06	0.38 ± 0.10	9.50 ± 4.88	3.91 ± 3.33	14.08 ± 9.82	(1)
83	HD 93205	287.57	−0.71	O3V	3187	0.38	1.24 ± 0.12	2.21 ± 0.11	5.82 ± 0.44	1.79 ± 0.27	3.25 ± 4.50	(13)
84is	HD 93222	287.74	−1.02	O7III((f))	2201	0.33	1.67 ± 0.12	1.58 ± 0.15	4.79 ± 0.60	0.95 ± 0.16	1.68 ± 5.35	(13)
85i	HD 93521	183.14	+62.15	O9Vp	1760	0.04	⋯	0.058 ± 0.01	1.45 ± 0.61	⋯	21.18 ± 21.01	(14)
86	HD 93843	228.24	−0.90	O6III	2548	0.27	1.05 ± 0.15	0.79 ± 0.10	2.93 ± 0.48	0.75 ± 0.20	3.51 ± 5.16	(1)
87	HD 94493	289.01	−1.18	B0.5Iab	3888	0.23	0.82 ± 0.14	0.72 ± 0.10	3.13 ± 0.57	0.88 ± 0.27	0.79 ± 5.07	(1)
88	HD 99857	294.78	−4.94	B1Ib	3058	0.33	1.10 ± 0.13	0.59 ± 0.10	1.79 ± 0.36	0.54 ± 0.16	4.79 ± 5.93	(1)
89	HD 99890	291.75	+4.43	B0.5V:	3070	0.24	0.72 ± 0.10	1.00 ± 0.10	4.17 ± 0.59	1.39 ± 0.34	−5.89 ± 10.60	(1)
90	HD 100340	258.85	+61.23	B1V	3000	0.04	⋯	0.39 ± 0.1	9.75 ± 4.94	⋯	3.74 ± 7.57	(15)

Table 1. continued.

N (1)	Star (2)	l (3)	b (4)	Spectrum (5)	D, pc (6)	E(B − V) (7)	A_V (8)	P, % (9)	P/E(B − V), % (10)	P/A_V, % (11)	[Fe(rest)/H]$_d$ (12)	Reference (13)
91	HD 103779	296.85	−1.02	B0.5II	3061	0.21	0.69 ± 0.12	0.690 ± 0.005	3.29 ± 0.18	1.00 ± 0.19	2.54 ± 5.59	(1)
92	HD 104705	297.45	−0.34	B0.5III	2082	0.28	1.22 ± 0.10	0.820 ± 0.1	2.93 ± 0.46	0.67 ± 0.14	0.91 ± 6.05	(1)
93	HD 106490	298.23	+3.79	B2IV	110	0.06	· · ·	· · ·	· · ·	· · ·	12.21 ± 7.60	
94	HD 108248	300.13	−0.36	B0.5IV	100	0.20	· · ·	· · ·	· · ·	· · ·	3.23 ± 12.66	
95	HD 108639	300.22	+1.95	B1III	110	0.35	· · ·	1.87 ± 0.10	5.34 ± 0.44	· · ·	· · ·	(1)
96	HD 109399	301.71	−9.88	B1Ib	1900	0.26	0.81 ± 0.11	2.19 ± 0.10	8.42 ± 0.71	2.70 ± 0.49	5.81 ± 5.24	(1)
97ms	HD 110432	301.96	−0.20	B0.5IIIe	301	0.51	2.01 ± 0.35	2.02 ± 0.102	3.96 ± 0.28	1.00 ± 0.22	· · ·	(5)
98	HD 111934	303.20	+2.51	B2Ib	2525	0.51	1.25 ± 0.13	· · ·	· · ·	· · ·	· · ·	
99mv	HD 113904	304.67	−2.49	WC5+B0Ia	2660	0.21	0.76 ± 0.07	1.54 ± 0.01	7.33 ± 0.40	2.02 ± 0.20	· · ·	(7)
100ms	HD 114886	305.52	−0.83	O9IIIn	1000	0.29	0.84 ± 0.08	2.03 ± 0.13	7.00 ± 0.69	2.41 ± 0.37	· · ·	(5)
101	HD 115071	305.76	+0.15	B0.5V	1200	0.44	· · ·	1.87 ± 0.10	4.25 ± 0.32	· · ·	· · ·	(1)
102i	HD 116658	316.11	+50.84	B1III-IV	80	0.14	· · ·	0.09 ± 0.01	0.64 ± 0.12	· · ·	24.66 ± 21.91	(14)
103s	HD 116781	307.05	−0.07	B0IIIe	1492	0.34	1.40 ± 0.14	1.46 ± 0.10	4.29 ± 0.42	1.04 ± 0.18	3.79 ± 5.95	(1)
104	HD 116852	304.88	−16.13	O9III	4832	0.21	0.51 ± 0.10	· · ·	· · ·	· · ·	3.38 ± 6.09	
105	HD 119608	320.35	+43.13	B1Ib	4200	0.12	· · ·	0.440 ± 0.035	3.67 ± 0.60	· · ·	· · ·	(1)
106	HD 121263	314.07	+14.19	B2.5IV	120	0.05	· · ·	0.070 ± 0.035	1.40 ± 0.98	· · ·	17.50 ± 6.84	(1)
107	HD 121968	333.97	+55.84	B1V	3800	0.15	· · ·	0.410 ± 0.121	2.73 ± 0.99	· · ·	· · ·	(1)
108m	HD 122879	312.26	+1.79	B0Ia	2265	0.36	1.13 ± 0.14	1.93 ± 0.116	5.36 ± 0.47	1.70 ± 0.31	4.23 ± 6.04	(5)
109ms	HD 124314	312.67	−0.42	O6Vnf	1100	0.46	1.42 ± 0.17	2.32 ± 0.10	5.04 ± 0.33	1.63 ± 0.26	5.76 ± 4.76	(5)
110	HD 127972	322.77	+16.67	B1.5Vne	90	0.11	· · ·	· · ·	· · ·	· · ·	2.99 ± 8.44	
111ms	HD 135591	320.13	−2.64	O7.5IIIf	1250	0.22	0.79 ± 0.08	1.54 ± 0.084	7.00 ± 0.70	1.96 ± 0.29	· · ·	(5)
112	HD 136298	331.32	+13.82	B1.5IV	210	0.07	· · ·	· · ·	· · ·	· · ·	4.44 ± 8.38	
113s	HD 137595	336.72	+18.86	B3Vn	400	0.25	· · ·	· · ·	· · ·	· · ·	· · ·	
114	HD 138690	333.19	+11.89	B2IV	130	0.07	· · ·	· · ·	· · ·	· · ·	19.35 ± 6.92	
115ms	HD 141637	346.10	+21.70	B2.5Vn	160	0.18	0.76 ± 0.17	0.81 ± 0.20	4.50 ± 1.36	1.07 ± 0.51	5.79 ± 4.55	(5)
116	HD 143018	347.21	+20.23	B1V	141	0.07	· · ·	0.348 ± 0.107	4.97 ± 2.24	· · ·	12.33 ± 4.38	(1)
117	HD 143118	338.77	+11.01	B2.5IV	140	0.02	· · ·	· · ·	· · ·	· · ·	18.77 ± 7.01	
118s	HD 143275	350.10	+22.49	B0.3IVe	123	0.21	0.65 ± 0.09	0.331 ± 0.036	1.58 ± 0.25	0.51 ± 0.13	7.99 ± 3.30	(1)
119m	HD 144217	353.19	+23.60	B0.5V	163	0.21	0.57 ± 0.09	0.84 ± 0.185	4.00 ± 1.07	1.47 ± 0.56	8.37 ± 1.79	(5)
120m	HD 144470	352.76	+22.76	B1V	183	0.22	0.82 ± 0.10	1.14 ± 0.017	5.18 ± 0.31	1.40 ± 0.20	6.67 ± 3.07	(5)
121s	HD 144965	339.04	+8.42	B2Vne	290	0.35	· · ·	· · ·	· · ·	· · ·	· · ·	
122v	HD 147165	351.33	+17.00	B1IIISB,V	137	0.41	1.48 ± 0.09	1.52 ± 0.01	3.71 ± 0.11	1.03 ± 0.07	6.60 ± 5.99	(16)
123	HD 147683	344.86	+10.09	B4V	280	0.39	· · ·	1.90 ± 0.10	4.87 ± 0.38	· · ·	· · ·	(1)
124mv	HD 147888	353.65	+17.71	B3V:SB	195	0.51	2.08 ± 0.11	3.51 ± 0.01	6.88 ± 0.15	1.69 ± 0.09	8.65 ± 3.88	(7)
125m	HD 147933	353.68	+17.70	B1.5V	118	0.47	2.07 ± 0.11	2.68 ± 0.01	5.70 ± 0.14	1.29 ± 0.08	6.78 ± 1.65	(7)
126vs	HD 148184	357.93	+20.68	B1.5Ve	160	0.44	2.00 ± 0.18	0.42 ± 0.10	0.95 ± 0.25	0.21 ± 0.07	8.54 ± 3.25	(17)
127	HD 148594	350.93	+13.94	B9:V	134	0.21	0.65 ± 0.09	· · ·	· · ·	· · ·	· · ·	
128mv	HD 149404	340.54	+3.01	O9Ia	908	0.62	2.19 ± 0.27	3.18 ± 0.10	5.13 ± 0.24	1.45 ± 0.23	· · ·	(5)
129ms	HD 149757	6.28	+23.59	O9.5Vnn	146	0.31	0.95 ± 0.09	1.48 ± 0.01	4.77 ± 0.19	1.55 ± 0.16	8.09 ± 1.33	(7)
130	HD 149881	31.37	+36.23	B0.5III	2100	0.11	· · ·	0.46 ± 0.03	4.18 ± 0.65	· · ·	15.81 ± 26.69	(1)
131i	HD 151804	343.62	+1.94	O8Iab	1254	0.30	1.30 ± 0.13	0.90 ± 0.10	3.00 ± 0.43	0.69 ± 0.15	5.51 ± 7.34	(18)
132	HD 151805	343.20	+1.59	B1Ib	6009	0.43	1.41 ± 0.16	· · ·	· · ·	· · ·	· · ·	
133m	HD 152236	343.03	+0.87	B1Ia	612	0.60	2.24 ± 0.27	2.44 ± 0.035	4.07 ± 0.13	1.09 ± 0.15	· · ·	(5)
134iv	HD 152590	344.84	+1.83	O7.5V	1800	0.46	1.51 ± 0.17	0.737 ± 0.100	1.60 ± 0.25	0.49 ± 0.12	4.61 ± 3.71	(12)
135	HD 154368	349.97	+3.22	O9Ib	1046	0.76	2.53 ± 0.15	0.308 ± 0.007	0.41 ± 0.01	0.12 ± 0.01	· · ·	(1)

Table 1. continued.

N (1)	Star (2)	l (3)	b (4)	Spectrum (5)	D, pc (6)	$E(B-V)$ (7)	A_V (8)	P, % (9)	$P/E(B-V)$, % (10)	P/A_V, % (11)	$[Fe(rest)/H]_d$ (12)	Reference (13)
136is	HD 155806	352.59	+2.87	O7.5Ve	860	0.28	0.69 ± 0.56	0.742 ± 0.090	2.65 ± 0.42	1.07 ± 1.00	5.38 ± 6.89	(12)
137s	HD 156110	70.99	+35.91	B3Vn	720	0.03	· · ·	0.74 ± 0.20	24.67 ± 14.89	· · ·	· · ·	(1)
138m	HD 157246	334.64	−11.48	B1Ib	348	0.06	0.17 ± 0.05	0.90 ± 0.1	15.00 ± 4.17	5.32 ± 2.04	15.65 ± 9.15	(5)
139	HD 157857	12.97	+13.31	O7V	1902	0.43	1.48 ± 0.13	2.40 ± 0.20	5.58 ± 0.59	1.62 ± 0.28	· · ·	(1)
140	HD 158926	351.74	−2.21	B2IV	220	0.10	· · ·	· · ·	· · ·	· · ·	12.14 ± 4.72	
141	HD 160578	351.04	−4.72	B1.5III	142	0.08	· · ·	0.250 ± 0.035	3.13 ± 0.83	· · ·	8.73 ± 9.70	(1)
142ms	HD 164740	5.97	−1.17	O7.5V(n)	1330	0.86	4.48 ± 0.14	7.35 ± 0.1	8.55 ± 0.22	1.64 ± 0.07	· · ·	(5)
143m	HD 165024	343.33	−13.82	B2Ib	250	0.05	0.17 ± 0.07	1.02 ± 0.035	20.40 ± 4.78	5.96 ± 2.62	16.83 ± 8.40	(5)
144s	HD 165955	357.41	−7.43	B1Vnp	1640	0.21	· · ·	1.19 ± 0.10	5.67 ± 0.75	· · ·	· · ·	(1)
145	HD 167264	10.46	−1.74	B0.5Ia	1514	0.30	0.98 ± 0.13	0.466 ± 0.033	1.55 ± 0.16	0.48 ± 0.09	· · ·	(1)
146	HD 167756	351.47	−12.30	B0.5Iab?	4230	0.07	· · ·	0.460 ± 0.005	6.57 ± 1.01	· · ·	20.42 ± 12.55	(1)
147	HD 168076	16.94	+0.84	O5V	1820	0.76	2.64 ± 0.13	2.58 ± 0.20	3.39 ± 0.31	0.98 ± 0.12	· · ·	(1)
148m	HD 170740	21.06	−0.53	B2V	235	0.47	1.37 ± 0.09	2.09 ± 0.20	4.45 ± 0.52	1.53 ± 0.25	· · ·	(5)
149	HD 175360	12.53	−11.29	B6III	270	0.12	· · ·	0.396 ± 0.0329	3.30 ± 0.55	· · ·	· · ·	(3)
150	HD 177989	17.81	−11.88	B2II	5021	0.22	0.63 ± 0.09	0.88 ± 0.20	4.00 ± 1.09	1.40 ± 0.52	6.44 ± 4.85	(1)
151mv	HD 179406	28.23	−8.31	B3IVvar	227	0.31	0.89 ± 0.09	1.30 ± 0.03	4.19 ± 0.23	1.46 ± 0.18	· · ·	(7)
152ms	HD 184915	31.77	−13.29	B0.5IIIne	700	0.22	0.68 ± 0.07	1.39 ± 0.331	6.32 ± 1.79	2.06 ± 0.70	· · ·	(5)
153	HD 185418	53.60	−2.17	B0.5 V	1027	0.47	1.17 ± 0.09	0.74 ± 0.20	1.57 ± 0.46	0.63 ± 0.22	8.86 ± 4.26	(1)
154	HD 186994	78.62	+10.06	B0III	2500	0.16	0.53 ± 0.08	0.74 ± 0.20	4.63 ± 1.54	1.41 ± 0.60	· · ·	(1)
155	HD 188209	80.99	+10.09	O9.5Ib	2210	0.15	0.68 ± 0.11	0.274 ± 0.0288	1.83 ± 0.31	0.40 ± 0.11	· · ·	(3)
156s	HD 190918	72.65	+2.06	WN4+O9.7Iab	2290	0.41	· · ·	0.470 ± 0.032	1.15 ± 0.11	· · ·	· · ·	(1)
157s	HD 192035	83.33	+7.76	B0III-IVn	2800	0.35	· · ·	1.473 ± 0.0559	4.21 ± 0.28	· · ·	· · ·	(3)
158iv	HD 192639	74.90	+1.48	O8V	999	0.61	1.92 ± 0.13	0.2 ± 0.1	0.33 ± 0.17	0.10 ± 0.06	6.97 ± 4.79	(18)
159	HD 195965	85.71	+5.00	B0V	1300	0.22	0.68 ± 0.10	1.01 ± 0.20	4.59 ± 1.12	1.49 ± 0.51	9.70 ± 10.08	(1)
160	HD 197512	87.89	+4.63	B1V	1614	0.29	0.70 ± 0.07	1.145 ± 0.0654	3.95 ± 0.36	1.62 ± 0.25	· · ·	(3)
161m	HD 198478	85.75	+1.49	B3Ia	890	0.57	1.48 ± 0.13	2.68 ± 0.02	4.70 ± 0.12	1.81 ± 0.18	· · ·	(7)
162	HD 198781	99.94	+12.61	B2IV	768	0.31	0.80 ± 0.07	1.38 ± 0.20	4.45 ± 0.79	1.73 ± 0.41	· · ·	(1)
163	HD 199579	87.50	−0.30	B0.5V	990	0.33	1.01 ± 0.09	0.88 ± 0.20	2.67 ± 0.69	0.87 ± 0.27	· · ·	(1)
164	HD 201345	78.44	−9.54	O9V	2570	0.17	· · ·	0.183 ± 0.0688	1.08 ± 0.47	· · ·	· · ·	(3)
165	HD 202347	88.22	−2.08	B1V	1300	0.19	0.53 ± 0.08	0.271 ± 0.0659	1.43 ± 0.42	0.51 ± 0.21	17.75 ± 8.57	(3)
166s	HD 202904	80.98	−10.05	B2Vne	276	0.13	· · ·	0.33 ± 0.05	2.54 ± 0.58	· · ·	7.47 ± 11.56	(1)
167s	HD 203374	100.51	+8.62	B0IVpe	820	0.60	1.88 ± 0.21	0.37 ± 0.20	0.62 ± 0.34	0.20 ± 0.13	7.26 ± 8.34	(1)
168m	HD 203532	309.46	−31.74	B5V	211	0.28	0.94 ± 0.10	1.37 ± 0.035	4.89 ± 0.30	1.45 ± 0.19	· · ·	(5)
169v	HD 206267	99.29	+3.74	O6V	814	0.52	1.47 ± 0.11	1.27 ± 0.06	2.44 ± 0.16	0.87 ± 0.11	9.29 ± 4.24	(19)
170	HD 206773	99.80	+3.62	B0V	597	0.45	1.99 ± 0.16	2.03 ± 0.20	4.51 ± 0.54	1.02 ± 0.18	· · ·	(1)
171m	HD 207198	103.14	+6.99	O9II	1216	0.54	1.50 ± 0.22	0.98 ± 0.01	1.81 ± 0.05	0.66 ± 0.10	10.01 ± 3.57	(7)
172s	HD 207308	103.11	+6.82	B0.7III-IVn	1470	0.52	1.61 ± 0.19	0.88 ± 0.20	1.69 ± 0.42	0.55 ± 0.19	9.25 ± 4.15	(1)
173mv	HD 207538	101.60	+4.67	O9.5V	880	0.64	1.44 ± 0.21	2.24 ± 0.03	3.50 ± 0.10	1.56 ± 0.25	9.43 ± 4.16	(8)
174	HD 208440	104.03	+6.44	B1V	620	0.34	· · ·	1.287 ± 0.0559	3.79 ± 0.28	· · ·	· · ·	(3)
175	HD 208947	106.55	+9.00	B2V	500	0.19	0.63 ± 0.18	0.51 ± 0.20	2.68 ± 1.19	0.81 ± 0.55	· · ·	(1)
176	HD 209339	104.58	+5.87	B0IV	980	0.35	1.09 ± 0.14	1.66 ± 0.20	4.74 ± 0.71	1.53 ± 0.38	6.09 ± 4.48	(1)
177m	HD 210121	56.88	−44.46	B9V	223	0.38	0.76 ± 0.08	1.32 ± 0.04	3.47 ± 0.20	1.73 ± 0.23	· · ·	(20)
178iv	HD 210809	99.85	−3.13	O9Ib	3961	0.31	1.05 ± 0.13	0.6 ± 0.1	1.94 ± 0.39	0.57 ± 0.17	· · ·	(18)
179iv	HD 210839	103.83	+2.61	O6Iab	1260	0.57	1.15 ± 0.17	1.4 ± 0.1	2.46 ± 0.22	1.22 ± 0.26	8.35 ± 4.21	(18)
180	HD 212791	101.64	−4.30	B8	370	0.06	· · ·	1.183 ± 0.0572	19.72 ± 4.24	· · ·	· · ·	(3)

Table 1. continued.

N (1)	Star (2)	l (3)	b (4)	Spectrum (5)	D, pc (6)	E(B − V) (7)	A_V (8)	P, % (9)	P/E(B − V), % (10)	P/A_V, % (11)	[Fe(rest)/H]$_d$ (12)	Reference (13)
181m	HD 214680	96.65	−16.98	O9V	610	0.08	0.21 ± 0.08	0.55 ± 0.124	6.88 ± 2.41	2.62 ± 1.58	13.96 ± 10.46	(9)
182	HD 214993	97.65	−16.18	B1.5IIIn	610	0.10	0.50 ± 0.13	0.467 ± 0.0309	4.67 ± 0.78	0.93 ± 0.30	17.12 ± 10.12	(3)
183	HD 215733	85.16	−36.35	B1II	2900	0.10	⋯	0.24 ± 0.03	2.40 ± 0.54	⋯	16.44 ± 18.39	(1)
184	HD 218376	109.96	−0.79	B1III	383	0.23	0.71 ± 0.10	0.84 ± 0.20	3.65 ± 1.03	1.18 ± 0.45	5.02 ± 6.93	(1)
185s	HD 218915	108.06	−6.89	O9.5Iabe	3660	0.26	0.70 ± 0.39	1.08 ± 0.20	4.15 ± 0.93	1.53 ± 1.13	⋯	(1)
186	HD 219188	83.03	−50.17	B0.5III	1064	0.08	⋯	0.147 ± 0.0527	1.84 ± 0.89	⋯	⋯	(3)
187	HD 220057	112.13	+0.21	B2IV	1421	0.24	0.56 ± 0.08	0.75 ± 0.20	3.13 ± 0.96	1.34 ± 0.54	⋯	(1)
188	HD 224151	115.44	−4.64	B0.5II-III	1355	0.42	1.45 ± 0.16	0.567 ± 0.120	1.35 ± 0.32	0.39 ± 0.13	4.73 ± 5.03	(1)
189	HD 224572	115.55	−6.36	B1V	340	0.19	0.51 ± 0.17	1.255 ± 0.119	6.61 ± 0.97	2.45 ± 1.05	19.06 ± 8.75	(1)
190	HD 232522	130.70	−6.71	B1II	5438	0.21	0.64 ± 0.12	1.61 ± 0.18	7.67 ± 1.22	2.51 ± 0.74	⋯	(1)
191v	HD 303308	287.59	−0.61	O3V	3631	0.45	1.36 ± 0.12	3.10 ± 0.12	6.89 ± 0.42	2.28 ± 0.30	4.24 ± 5.53	(13)
192m	HD 308813	294.79	−1.61	O9.5V	2398	0.28	⋯	1.85 ± 0.03	6.61 ± 0.34	⋯	⋯	(21)
193s	BD +35 4258	77.19	−4.74	B0.5 Vn	3093	0.25	0.72 ± 0.08	0.51 ± 0.18	2.04 ± 0.80	0.70 ± 0.33	4.34 ± 6.57	(1)
194s	BD +53 2820	101.24	−1.69	B0IV:n	4506	0.37	1.08 ± 0.09	2.30 ± 0.18	6.22 ± 0.65	2.13 ± 0.34	⋯	(1)
195v	CPD -59 2603	287.59	−0.69	O7V	2630	0.46	1.45 ± 0.17	1.97 ± 0.13	4.28 ± 0.38	1.36 ± 0.25	25.27 ± 9.16	(13)
196s	CPD -69 1743	303.71	−7.35	B1Vn	4700	0.30	⋯	0.88 ± 0.10	2.93 ± 0.43	⋯	⋯	(1)

Notes. 'v' — variable star; 's' — star with peculiar spectrum; 'm' — maximum polarization P_{max} (wavelength dependence of polarization is known); 'i' — interstellar polarization;
References for observational data: (1) Heiles (2000); (2) Ghosh et al. (1999); (3) this paper; (4) Anderson & Wannier (1997); (5) Serkowski et al. (1975); (6) Roche et al. (1997);
(7) Efimov (2009); (8) Martin et al. (1999); (9) Mcdavid (2000); (10) Leroy & Le Borgne (1987); (11) Oudmaijer & Drew (1999); (12) Vink et al. (2009); (13) Marracco et al. (1993);
(14) Berdyugin et al. 2010, in preparation; (15) Weitenbeck (2008); (16) Das et al. (2010); (17) Poeckert et al. (1979); (18) Harries et al. (2002); (19) Elias et al. (2008);
(20) Larson et al. (1996); (21) Vega et al. (1994).

Voshchinnikov et al.: Interstellar polarization and grain alignment